Journal of the Korea Institute for Structural Maintenance and Inspection
Vol. 22, No. 1, January 2018, pp.199-207
https://doi.org/10.11112/jksmi.2018.22.1.199
pISSN 2234-6937
eISSN 2287-6979

이중 보강근을 가지는 FRC 보의 휨성능

김성은[1], 김승훈[2*]

Flexural Behavior of Fiber Reinforced Concrete Beams with Hybrid Double-layer Reinforcing Bars

Seongeun Kim[1], Seunghun Kim[2*]

Abstract: Experimental programs were performed to evaluate the flexural performance of fiber reinforced concrete(FRC) beams using a hybrid double-layer arrangement of steel bars and fiber reinforced polymer(FRP) bars or using FRP bars only. A total of seven beam specimens were produced with type of tensile reinforcing bar(CFRP bar, GFRP bar, steel bar) and the poly vinyl alcohol(PVA) fiber mixing ratio(0.5%, 0%) as variable. An analysis method for predicting the flexural behaviors of FRC beams with hybrid arrangement of heterogeneous reinforcing bars through finite element analysis was proposed and verified. In case of the specimens with the double-layer reinforcing bars, the test results showed that the first cracking load of specimen with a double-layer arrangement of steel bars was greater by 26-34% than specimens with a hybrid double-layer arrangement of steel and FRP bars. In maximum flexural strengths, the specimen that used CFRP bars as bottom tensile reinforcing bar showed the greatest strength among the specimens with the double-layer reinforcing bars. When the maximum moment value obtained through experiments was compared with that obtained through analysis, the ratio was 1.2 on average, the standard deviation was 0.085, and the maximum error rate was 22% or less. Based on these results, the finite element analysis model proposed in this study can effectively simulate the actual behavior of the beams with hybrid double-layer reinforcing bars.

Keywords: FRP bar, Flexural performance, PVA fiber, Finite element analysis

1. Introduction

Steel bars that are frequently used in reinforced concrete (RC) structures have the problem of durability loss due to corrosion by chloride attack or neutralization. FRP (Fiber Reinforced Polymers) As a solution, the use of fiber reinforced polymer (FRP) bars with corrosion resistance feature is increasing. FRP bars are expected to provide an effective alternative to the prevention of durability degradation due to aging of structures and the repair and reinforcement of aged structures because they have excellent features such as lightweight, low thermal conductivity, and high strength.

However, FRP bars require special care because they are brittle unlike steel reinforcing bars when used on concrete members. The failure modes of concrete flexural members reinforced with FRP bars are distinguished by the reinforcing bar ratio. Compressive failure of concrete occurs if the reinforcing bar ratio of FRP bar is higher than the balanced reinforcing bar ratio, and fracture of FRP bar occurs before concrete failure if the reinforcing bar ratio of FRP bar is lower than the balanced reinforcing bar ratio (ACI 440.1R-15, 2015). Most design codes and guides recommend the excessive reinforcement of FRP bars to ensure the plastic deformation of concrete and improve the ductility (ACI 440.1R-15, 2015; CEB-FIP, 1993; CAN/CSA S806-02, 2002; JSCE, 1997).

Furthermore, the modulus of elasticity of FRP bars is smaller than that of steel reinforcing bars except for some highly elastic carbon FRP (CFRP) bars. Thus, structures reinforced with FRP bars generate a greater crack width and deflection than RC structures that have the same reinforcing bar ratio. As a solution, fiber reinforced concrete (FRC) members can be used by mixing concrete with poly vinyl alcohol (PVA) fibers that are distributed with multiple micro-cracks under a flexural stress. In addition, a hybrid double-layer arrangement specification

[1]정회원, 한밭대학교 건축공학과 대학원 석사과정
[2]정회원, 한밭대학교 건축공학과 교수, 교신저자
***Corresponding author:** kimsh@hanbat.ac.kr
Department of Architectural Engineering, Hanbat National University, 125 Dongseodero, Yuseong-gu, Daejeon 31458, Korea
• 본 논문에 대한 토의를 2018년 2월 1일까지 학회로 보내주시면 2018년 3월호에 토론결과를 게재하겠습니다.

of FRP and steel bars appears if the outer surface of an existing RC structure is reinforced with FRP bars or if FRP bars are used in the part close to the outer surface of the member and steel bars are used in the part far from it. Such hybrid arrangement specification of steel and FRP bars has advantages because the rigidity of the flexural members is increased by complementing the low modulus of elasticity of FRP bars with steel bars and the durability and constructability are improved through FRP bars (Yoon et al., 2011; Kim et al., 2016).

The flexural member design methods of RC structures using steel bars and concrete structures using FRP bars show many differences in the calculation of flexural strength, deflection, and strength reduction coefficients. Thus, in the RC members that use steel and FRP bars in combination, it is difficult to predict the flexural performance with the existing design methods; experiments and analytical research are being conducted on this, but they are still in the nascent stage (Yoon et al., 2011; Kim et al., 2016; Aiello et al., 2002; Yang et al., 2011). Especially the research on the flexural performance of FRC members with hybrid arrangement of steel and FRP bars is insufficient. Therefore, in this study, flexural tests were conducted to evaluate the flexural performance of FRC beams with a hybrid arrangement of steel and FRP bars and FRC beams using FRP bars only. In addition, an analysis method for predicting the flexural behavior and cracks of FRC beams with hybrid arrangement of heterogeneous reinforcing bars through finite element analysis was proposed and verified.

2. Analysis of Precedent Studies

The important results of existing studies conducted to evaluate the flexural performance of RC members with a hybrid arrangement of steel and FRP bars can be summarized as follows.

Aiello and Ombres (2002) evaluated the flexural performance of concrete beams with a combination of Aramid FRP (AFRP) bars and steel bars. The steel and AFRP bars were arranged in a single layer on the same line in the tensile section of the beam or in double layers by placing the steel bar on top of AFRP bar. The experimental results showed that the additional arrangement of steel bar on the concrete section reinforced with AFRP bar significantly increased the ductility of structure and reduced the width and gaps of cracks. However, the contribution of the additionally arranged steel bar to the flexural performance did not exceed 15%.

Yang et al. (2011) fabricated 10 specimens and conducted experiments with them to examine the behaviors of beams with a hybrid arrangement of FRP and steel bars. They analyzed such behaviors as crack patterns, rigidity after cracking, deflection, and ductility. Their experimental results showed that the hybrid arrangement of heterogeneous reinforcing bars could control large deflection, crack depth and width.

Leung and Balendran (2003) investigated the flexural response of RC beams with glass FRP (GFRP) bars and steel bars arranged on different lines. They reported that the beam with a hybrid reinforcement specification showed a greater flexural strength than the beam reinforced with steel or GFRP bars only and analyzed that in the case of the beam with a hybrid reinforcement specification, the GFRP bar increased the flexural strength after the steel bar yielded.

3. Experiment

3.1 Experimental Design and Method

A flexural experiment was planned to evaluate the effect of the reinforcing bar specifications such as steel bar, FRP bar, and the hybrid arrangement of steel and FRP bars on the flexural strength of FRC members. Table 1 lists the specimens and Fig. 1 shows the detailed diagrams of specimens. As shown

Table 1 Detail of specimens

Speci-men	b(mm) × h(mm)	PVA (%)	Tensile Reinforcing bar		
			Type-number-diameter	Area, As (mm^2)	ρ
P1-SS			SD400-2 -16 mm	397.2	0.0042
P1-SG	200 × 300	0.5	GFRP-2 -19 mm	573.0	0.0096
P1-SC			CFRP-2 -13 mm	253.4	0.0042
P0-C		0	CFRP-2 -13 mm	253.4	0.0096
P1-C	200 × 300	0.5	CFRP-2 -13 mm	253.4	0.0096
P0-G		0	GFRP-2 -19 mm	573.0	0.0042
P1-G		0.5	GFRP-2 -19 mm	573.0	0.0042

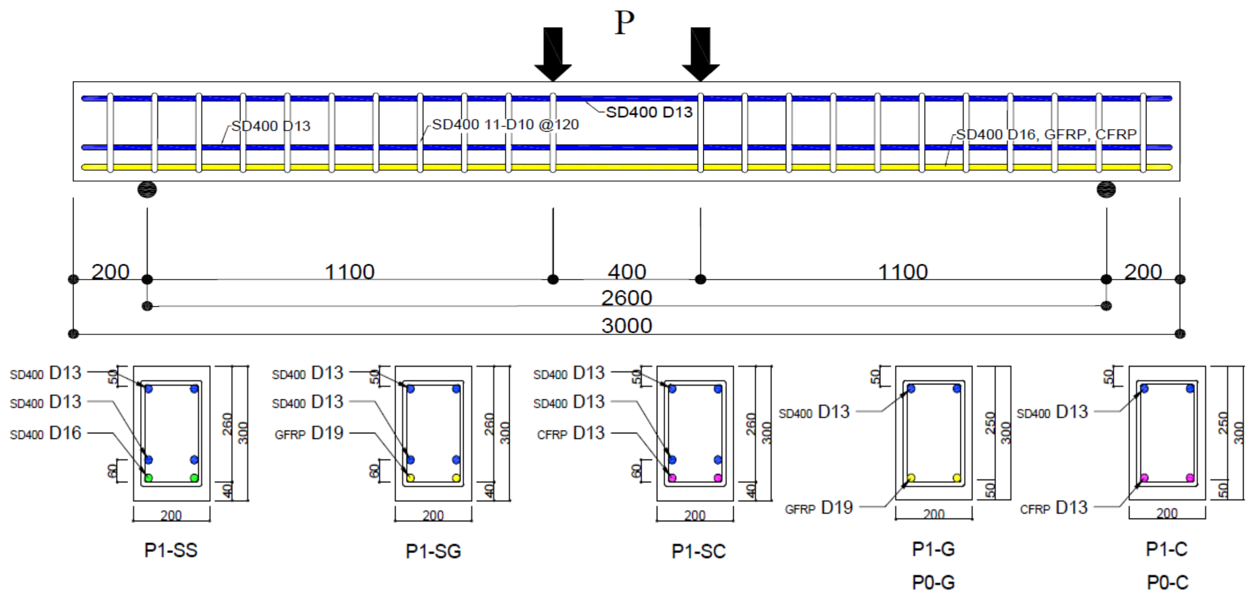

Fig. 1 Detailed view of the beam and specimen cross-section

Fig. 2 Specimen installation appearance

in Table 1. a total of seven beam specimens were fabricated with the type of tensile reinforcing bar, mixing of PVA fiber, etc. as parameters.

The specimens were planned in two types: single-layer and double-layer arrangements depending on the placement of tensile reinforcing bars. The double-layer specimens mixed PVA fibers at 0.5% and placed steel bars on top and CFRP, GFRP, and steel bar at the bottom as flexural tension members. The single-layer specimens mixed PVA fibers in two ratios, 0.5% and 0%, to examine the effect of PVA fiber reinforcement, and placed CFRP and GFRP bars as flexural tension members. The specimens were designed with cross section of 200 mm×300 mm, length of 3000 mm, clear span of 2600 mm, depth of inner reinforcing bar as 200 mm, and the depth of outer reinforcing bar as 260 mm.

Every specimen was designed for failure by concrete crushing with an excessive reinforcement ratio. The D10 deformed bar was used for the shear reinforcing bar of the specimens, and the D13 deformed bar was used for the compressive bar and inner reinforcing bar. For the outer reinforcing bars, two pieces each of D16 deformed bar, GFRP D19, and CFRP D13 were arranged depending on the specimen.

The experiment was carried out using the universal testing machine (UTM) until every specimen was fractured by the compressive failure of concrete. Fig. 2 shows the installation of the specimens. For loading, the displacement control method was adopted for four-point support loading. Loading was ended when the load decreased by at least 30% after the maximum load. For the measurement of deflection and strain, the mid-span deflection was measured with a 100mm displacement meter and the strain of each reinforcing bar was measured by attaching a gauge to the center of every reinforcing bar.

3.2 Experimental Design and Method

The PVA fibers of N Company in South Korea were used in the specimens, and the physical properties of the PVA fibers evaluated by the manufacturer are outlined in Table 2. The design criterion strength is 35 MPa and 100 mm×200 mm concrete specimens were fabricated to perform standard compressive strength test according to the existence or absence of fiber

Table 2 Properties of PVA fiber

Type of fiber	Polyvinyl alcohol
Elastic modulus(GPa)	24.5
Tensile strength(MPa)	883
Ultimate elongation(%)	10
Density(kg/m^3)	1.3
Fiber diameter(μm)	26
Fiber length(mm)	6~12

Table 3 Concrete proportion

Concrete	Unit weight(kg/m^2)					Mixing ratio(%)	f_{cu} (MPa)
	W	C	S	G	AE	PVA	
Plain concrete	164	433	814	924	4.5	0.0	21.4
FRC	164	433	814	924	4.5	0.5	20.5

Table 4 Material properties of reinforcement

Material	d_r (mm)	A_r (mm^2)	E_r (GPa)	f_y (MPa)	f_{fu} (MPa)
STEEL-D10	9.5	71.3	172	480	595
STEEL-D13	12.7	253.4	249	491	629
STEEL-D16	15.9	397.2	182	487	597
GFRP-D19	19.1	573	48	·	1118
CFRP-D13	12.7	253.4	103	·	1655

reinforcement. The experiment results showed that the compressive strength of specimen was 20.5 MPa for fiber-reinforced specimens and 21.4 MPa for other specimens. The concrete mixing ratio is shown in Table 3.

To examine the material properties of steel and FRP bars used in this experiment, the material experiment was conducted in accordance with KS B 0801. Three experiments were performed for each material, and their average values were calculated to derive the resultant value. Table 4. shows the material test results.

4. Experimental Results and Discussion

4.1 Crack and Failure Patterns

The crack pattern during the failure of every specimen is illustrated in Fig. 3 Failure of all the specimens was done by concrete crushing as planned at first except for P1-C, which is a member using CFRP bars only and mixed with fibers. The P1-C specimen showed an initial behavior similar to other specimens mixed with fibers, but was failed by the CFRP bar fracture in the end (Fig. 3(f)). This seems to be due to the increased extreme compressive strain of the concrete reinforced with fibers. Recent studies related to fiber-reinforced concrete have reported that the extreme compressive strain of fiber-reinforced concrete was 0.0035 or higher. The concrete members reinforced with steel bars are generally designed around the yield point of steel bar. They do not consider the extreme compressive strain of concrete to be important during the member design because they assume that steel bars are yielded before the crushing failure of concrete. However, the extreme compressive strain of concrete plays a critical role in the prediction of the failure pattern for concrete members reinforced with FRP bars because they show linear elastic behavior with no yield point due to the nature of FRP. Therefore, when concrete reinforced with fibers and concrete reinforced with FRP bars are designed, the accurate extreme compressive strain of fiber-reinforced concrete is required to prevent the failure caused by the sudden fracture of FRP bars.

4.2 Load-Deflection Relationship

yielded before the crushing failure of concrete. However, the extreme compressive strain of concrete plays a critical role in the Fig. 4 shows the load-deflection relationship curve of the central part from the experimental results. Table 5. outlines the load and mid-span deflection at the first flexural crack and maximum load. In case of the specimens with the double-layer arrangement of steel and FRP bars (P1-SS, P1-SG, and P1-SC), the first cracking load of the P1-SS was greater by 26-34% than those of the P1-SG and P1-SC specimens. In case of the specimens with GFRP bar placed as the outermost reinforcing bar (P0-G, P1-G), the cracking load of the specimen with no fibers was higher by 16% than that of the specimen mixed with fibers. Furthermore, in the case of the specimens with CFRP bar placed as the outermost reinforcing bar (PO-C, P1-C), the first cracking load of the specimen with no fibers was higher by 18% than that of the specimen mixed with fibers. After cracking, the specimens with double-layer arrangement of FRP and steel bars showed a lower rigidity than the specimens reinforced with steel bars only.

As shown in Fig. 4(a), all the three specimens showed similar behavior of rigidity during the early cracking. After the

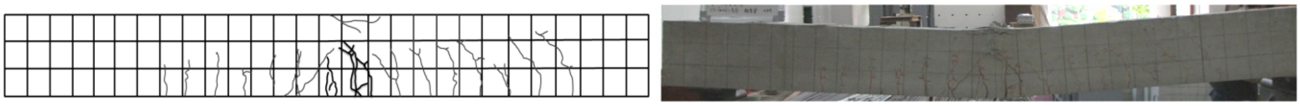

(a) P1-SS

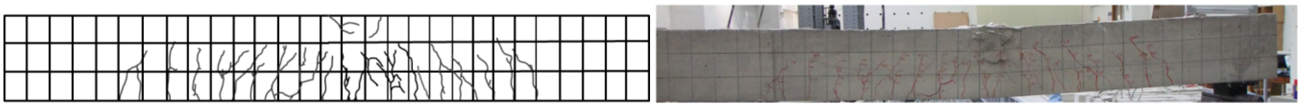

(b) P1-SG

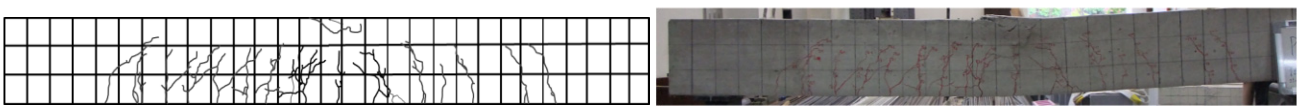

(c) P1-SC

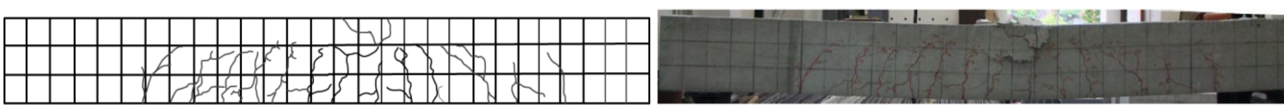

(d) P1-G

(e) P0-G

(f) P1-C

(g) P0-C

Fig. 3 Crack pattern of specimen

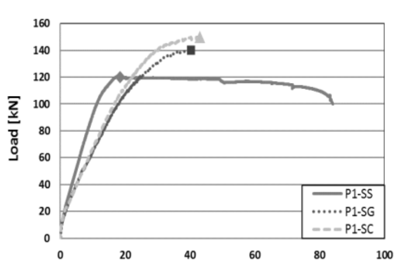

(a) Specimens P1-SS, P1-SG, P1-SC

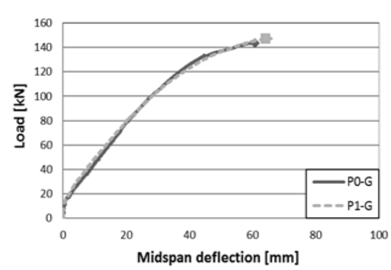

(b) Specimens P0-G, P1-G

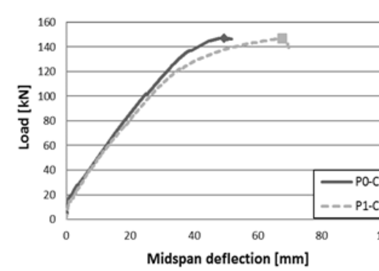

(c) Specimens P0-C, P1-C

Fig. 4 Loads-deflection relationship of specimens

first cracking, the rigidity of all specimens decreased. The specimen reinforced with steel bar only (P1-SS) showed a greater rigidity than the specimens reinforced with FRP bar as the outermost reinforcing bar (P1-SG, P1-SC). However, the P1-SS specimen showed a rapid decrease in rigidity after the steel bar yielded. When the maximum strengths of specimens were compared, the specimen where CFRP bar was arranged as the bottom tensile reinforcing bar (P1-SC) showed the greatest maximum strength among the specimens with a double-layer arrangement of steel and FRP bars. The other specimens did not

Table 5 Summary of test result

Specimen	P_{cr} (kN)	M_{cr} (kN·m)	P_u (kN)	M_u (kN·m)
P1-SS	18.87	10.38	120.86	66.47
P1-SG	14.91	8.20	140.28	77.24
P1-SC	14.05	7.73	149.82	82.40
P0-G	16.87	9.28	143.54	78.95
P1-G	14.53	7.99	147.39	81.06
P0-C	17.27	9.50	146.86	80.77

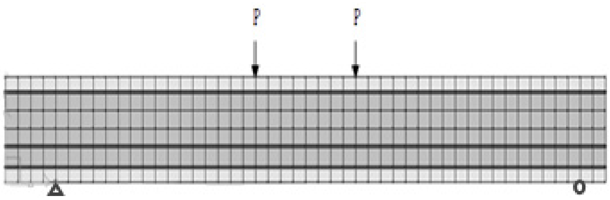

Fig. 5 FE model

show significant differences in rigidity and flexural strength depending on the mixing of fibers as shown in Fig. 4(b) and (c). However, the specimens mixed with fibers (P1-C, P1-G) showed a greater deflection under the maximum load than the specimens with no fibers (P0-C, P0-G), suggesting excellent strain performance. This difference was greater in the specimens using CFRP.

5. Finite Element Analysis

5.1 Finite Element Analysis Model

The VecTor2 program was used for finite element analysis. VecTor2 is a nonlinear finite element analysis program based on the modified compression field theory of concrete members. The finite element model is shown in Fig. 5 The external constraint of specimens was set as simple support and a vertical concentrated load was applied to the corresponding joint.

5.1.1 Concrete model

For the nonlinear material model of concrete used in this analysis, the stress-strain diagram Eq. (1) of general strength concrete range proposed by Popovics was used. The graphs (Fig. 6) reflect the fact that as the rigidity increases, the rising part shows linearity, and as the maximum compressive stress increases, the ductility of concrete decreases.

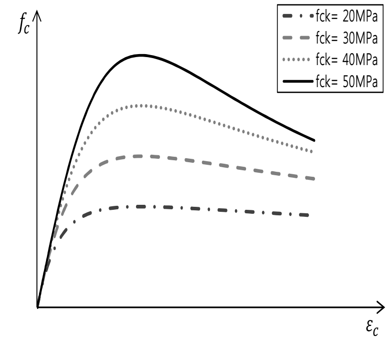

Fig. 6 FE model(concrete)

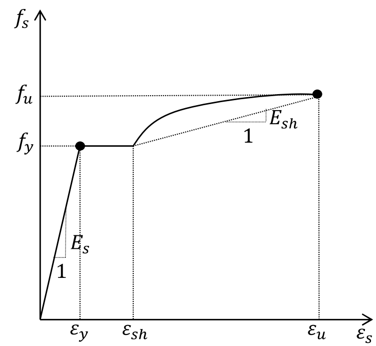

Fig. 7 FE model(reinforcement steel bar)

$$f_{ci} = \frac{\varepsilon_{ci}}{\varepsilon_P} f_P \frac{n}{n-1(\frac{\varepsilon_{ci}}{\varepsilon_P})} \quad \text{for } \varepsilon_{ci} < 0 \qquad (1)$$

Where f_P = corresponding to the peak compressive stress, ε_P = less compressive than the strain, n = The curve fitting parameter.

5.1.2 Reinforcing bar model

For steel bars, a model consisting of three parts of stress-strain curves (Fig. 7) was used. This analysis model shows a linear behavior until the steel bar reaches the yield point. Until fracture, the phase shows linear or nonlinear behavior depending on the parameter of hardening phenomenon. The tension and compressive reinforcement stress fs are determined by Eq. (2).

$$f_s = \begin{bmatrix} E_s\varepsilon_s & \text{for } \varepsilon_s < \varepsilon_y \\ f_y & \text{for } \varepsilon_y < \varepsilon_s < \varepsilon_{sh} \\ f_u + (f_y - f_u)\left(\dfrac{\varepsilon_u - \varepsilon_s}{\varepsilon_u - \varepsilon_{sh}}\right)^P & \text{for } \varepsilon_{sh} < \varepsilon_s < \varepsilon_u \\ 0 & \text{for } \varepsilon_u < \varepsilon_s \end{bmatrix} \qquad (2)$$

Where ε_s is the reinforcement strain, ε_y is the yield strain, ε_{sh}

is the strain at the onset of the strain hardening, ε_u is the ultimate strain, P is the strain-hardening parameter.

5.1.3 FRP bar model

The FRP bar is typically a brittle material. In other words, its independent behavior shows a linear behavior until failure and it suddenly fractures at failure. Therefore, the FRP bar was modeled with linear elasticity until its failure.

5.1.4 Contact model

The attachment model was assumed to be complete attachment. Furthermore, it was modeled with large values of rigidity and strength so as to prevent deformation in the combination of elements.

5.2 Comparison and Analysis of Finite Element Analysis Results

Fig. 8 shows graphs comparing the load-deflection relationship curves from the experiments of specimens and the finite element analysis results. In the case of specimens with a double-layer arrangement of steel and FRP bars (P1-SS, P1-SG, P1-SC), the graph from analysis showed somewhat greater initial rigidity compared to the graph from the experiment. In the case of the other four specimens (P0-G, P1-G, P0-C, P1-C), the time when the first crack occurs and the initial elastic zone section was predicted relatively accurately. For the specimen with a single-layer arrangement of GFRP bar as tensile reinforcing bar, the graph from analysis showed a smaller rigidity than the graph from experiment after the initial crack, but the difference is not large. For the specimen with a single-layer arrangement of CFRP bar as tensile reinforcing bar, the graph from analysis showed a somewhat greater rigidity than the graph from experiment after the initial crack, but the rigidity tended to decrease as it approached the maximum load. This difference in rigidity seems to be caused by the fact that the upward trend of extreme compressive strain of concrete depending on the mixing of PVA fibers affected the experimental results.

The experimental and analysis values of the crack moment and maximum moment of each specimen are outlined in Table 6. In the case of crack moment, the total error rate ranged between 0.97 and 1.07, indicating small variations. When the maximum moment values obtained through experiments were compared with the values obtained through finite element analysis, the ratio was 1.2 on average, the standard deviation was 0.085, and the maximum error rate was within 22%. These results suggest that the flexural reinforcing bar and PVA fibers had large effect on the crack and contraction of concrete, resulting in somewhat large maximum moment values. Based on this, it was concluded that the finite element analysis model proposed in this study simulates the actual behavior of the

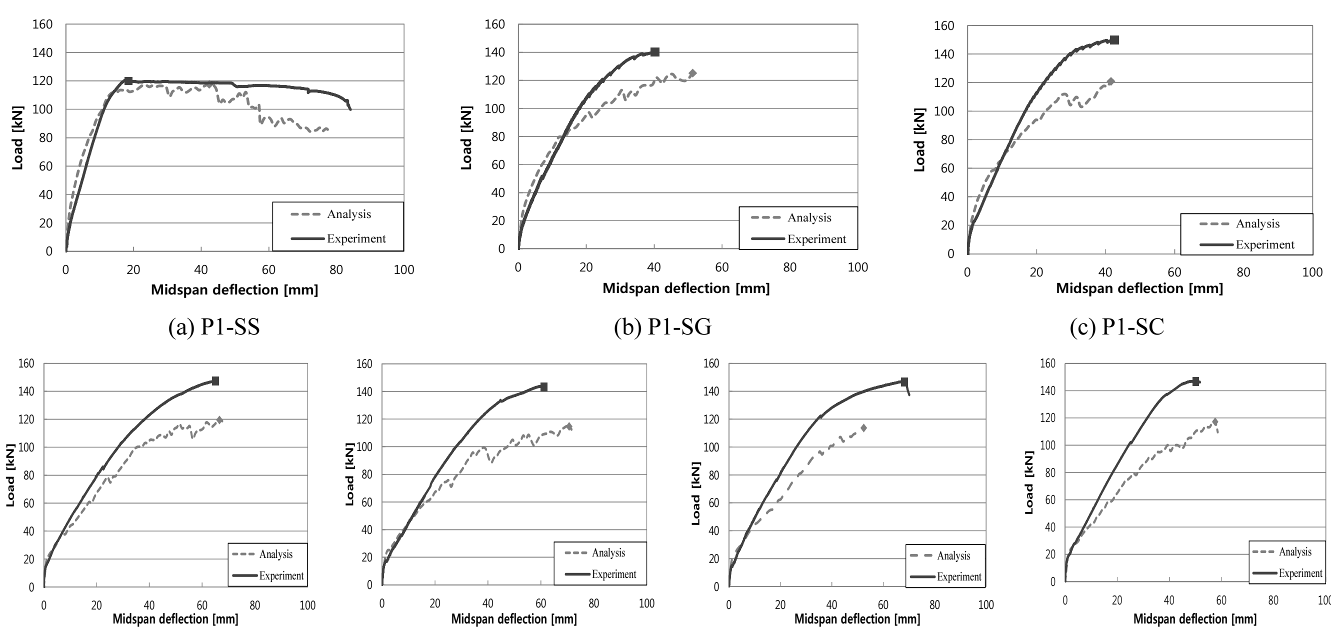

(a) P1-SS (b) P1-SG (c) P1-SC

(d) P1-G (e) P0-G (f) P1-C (g) P0-C

Fig. 8 Loads-deflection relationship of specimens

Table 6 The first crack moment and the experimental and analysis values of the maximum moment

Specimen	M_{cr} (kN·m)		M_{cr}_E/ M_{cr}_A	M_u (kN·m)		M_u_E/ M_u_A
	M_{cr} _E	M_{cr} _A		M_u _E	M_u_A	
P1-SS	10.38	10.56	0.98	66.47	64.68	1.03
P1-SG	8.20	7.92	1.04	77.24	68.86	1.12
P1-SC	7.73	7.21	1.07	82.40	66.99	1.23
P0-G	9.28	9.57	0.97	78.95	63.14	1.25
P1-G	7.99	8.14	0.98	81.06	65.73	1.23
P0-C	9.50	9.52	1.00	80.77	64.46	1.25
P1-C	8.02	8.20	0.98	80.25	62.54	1.28

beams reinforced with FRP bars and PVA fibers relatively accurately. However, further research is necessary to attain the reliability of the analysis model results in the case of various parameter analyses in future.

6. Conclusion

Flexural experiments were performed to evaluate the flexural performance of FRC beams using a hybrid arrangement of steel and FRP bars or using FRP bars only, with type of tensile reinforcing bar and the mixing or PVA fibers as the parameters. In addition, the applicability and reliability of a finite element analysis model were examined by conducting finite element analysis for the specimens. The following conclusions were derived from this study.

1) In the case of the specimens with a double-layer arrangement of steel and FRP bars (P1-SS, P1-SG, P1-SC), the initial cracking load of the specimens with steel bars only was higher than that of the specimens with a hybrid arrangement of steel and FRP bars. Furthermore, among the specimens with a single-layer arrangement, the specimens with no fibers (P0-G, P0-C) showed a higher initial cracking load than the specimens mixed with fibers (P1-G, P1-C)
2) For rigidity after cracking, the specimens with a hybrid arrangement of FRP and steel bars showed a lower rigidity than that of the specimens with steel bars only. Furthermore, when the maximum strengths of the specimens were compared, the specimen that arranged the CFRP bar as bottom tensile reinforcing bar (P1-SC) showed the greatest maximum strength among the specimens with a double-layer arrangement of steel and FRP bars.
3) The differences in rigidity and flexural strength depending on the mixing of fibers were not significant. However, the specimens mixed with fibers (P0-C, P0-G) showed greater deflections than the specimens with no fibers (P0-C, P0-G) under the maximum load, suggesting excellent strain performance.
4) The P1-C specimen was designed to fail by the concrete crushing fracture, but it failed by the fracture of the CFRP bar in the end. The reason for this seems to be the fact that the extreme compressive strain of the fiber-reinforced concrete increased. Therefore, the extreme compressive strain of concrete should be applied to prevent failure by sudden fracture of the FRP bar.
5) When the maximum moment value obtained through experiments was compared with that obtained through finite element analysis, the ratio was 1.2 on average, the standard deviation was 0.085, and the maximum error rate was within 22%. The main reason for the difference in the strength between the experiment and the finite element analysis is that the flexural reinforcing bars and PVA fibers affected the cracking and contraction of concrete in the experiment, resulting in a somewhat large maximum moment.

References

ACI 440.1R-15. (2015), Guide for the Design and Construction of Structural Concrete Reinforced with Fiber-Reinforced Polymer (FRP) Bars, American Concrete Institute.

Aiello, M. A., and Ombres, L. (2002), Structural performances of concrete beams with hybrid (fiber-reinforced polymer-steel) reinforcements, *Journal of Composites for Construction*, 6(2), 133-140.

Barris, C., Torres, L. I., Turon, A., Baena, M., and Catalan, A. (2009), An experimental study of the flexural behaviour of GFRP RC beams and comparison with prediction models. *Compos Struct*, 91 286–

295.
CAN/CSA S806-02. (2002), Design and Construction of Building Components with Fibre Reinforced Polymers, Canadian Standards Association.
CEB-FIP Model Code 90. (1990), Model code for concrete structures, Comite Euro-International du Beton, Bulletin, 213-214.
JSCE (1997), Recommendation for design and construction of concrete structures using continuous fiber reinforcing materials, JSCE Concrete Engineeering Series 23.
Kim, S. E., and Kim, S. H. (2016), Finite Element Analysis of Beams with FRP Bars and Steel Bars, *Conference Proceeding of Korea Concrete Institute*, 28(2), 83-84.
Leung, H. Y., and Balendran, R. V. (2003), Flexural behaviour of concrete beams internally reinforced with GFRP rods and steel rebars, *Structural Survey*, 21(4), 146-157.
Safan, M. A. (2013), Flexural behavior and design of steel-GFRP reinforced concrete beams, *ACI Materials Journal*, 110 (6), 677-685.
Shield, C., Galambos, T., and Gulbrandsen, P. (2011), On the History and Reliability of the Flexural Strength of FRP Reinforced Concrete Members in ACI 440.1R, *10th International Symposium on Fiber Reinforced Polymer Reinforcement for Concrete Structures, SP-275*, American Concrete Institute, 1-18.
Soliman, S. M., El-Salakawy, E., and Benmokrane, B. (2011), Bond performance of near-surface mounted FRP bars, *J Compos Constr*, 15(1), 103-111.
Yang, J. M., Yoo, D. Y., Shin, H. O., and Yoon, Y. S. (2011), Flexural Strength and Deflection Evaluation for FRP Bar Reinforced HSC Beams with Different Types of Reinforcing Bar and Fiber, *Journal of the Korea Concrete Institute*, 23(4), 413-420.
Yoon, Y. S., Yang, J. M., Min, K. H., and Shin, H. O. (2011), Flexural strength and deflection characteristics of high-strength concrete beams with hybrid FRP and steel bar reinforcement, American Concrete Institute, SP275, 57-77.
Yost, J. R., Gross, S. P., and Dinehart, D. W. (2003), Effective moment of inertia for glass fiberreinforced polymer-reinforced concrete beams, *ACI Struct. J.*, 100(6), 732-739.

Received : 12/18/2017
Revised : 12/19/2017
Accepted : 12/19/2017

요 지 : 이형철근과 FRP 보강근의 복합 이중근을 갖는 FRC 보의 휨성능을 평가하기 위하여 실험이 수행되었다. 인장근의 종류(CFRP 보강근, GFRP 보강근, 철근)과 PVA 섬유 혼입률(0.5%, 0%)을 주요변수로 한 7개의 실험체를 제작하였다. 유한요소해석을 통하여 FRC 보의 균열 및 휨거동을 예측하기 위한 해석적 방법이 제안되고 분석되었다. 복합 이중근을 가지는 실험체들에서 철근으로 이중근을 가지는 실험체가 철근과 FRP 보강근을 이단으로 배치한 실험체들에 비하여 26~34% 균열하중이 큰 것으로 나타났다. 최대 휨강도에서는 복합 이중근을 가지는 실험체들 중 CFRP 보강근을 최외측으로 한 실험체가 가장 큰 내력을 나타내었다. 해석과 실험을 통한 휨강도를 비교한 결과, 강도비는 평균 1.2, 표준편차 0.085, 최대 오차율은 22% 등으로 나타났다. 이러한 결과에서 본 연구의 유한요소해석방법이 복합 이중근을 가지는 보의 실제 거동을 효과적으로 표현할 수 있음을 알 수 있다.

핵심용어 : FRP 보강근, 휨성능, PVA 섬유, 유한요소해석